Co-occurrence of Noonan and Cardio-facio-cutaneous syndrome features in a patient with *KRAS* variant

Fernando Rodríguez,[1] Carla Vallejos,[1] Víctor M. Bolanos-Garcia,[2] Diana Ponce,[1] Nancy Unanue,[1] Francisco Garay,[3] Fernando Cassorla,[1] Mariana Aracena [3-4]

[1]Institute of Maternal and Child Research, School of Medicine, University of Chile Santiago, Chile

[2] Faculty of Health and Life Sciences, Department of Biological and Medical Sciences, Oxford Brookes University. Oxford, United Kingdom.

[3] División de Pediatría, Facultad de Medicina, Pontificia Universidad Católica de Chile,

[4] Unidad de Genética, Hospital Dr. Luis Calvo Mackenna, Santiago, Chile

Running title: *KRAS* mutation in Noonan syndrome

Correspondence to: Fernando Rodríguez

Address: Santa Rosa 1234, Santiago (8360160), Santiago, Chile.

Telephone: +56 - 2 – 29770855

Fax number: +56 - 2 - 24248240

E-mail address: frodriguezr@med.uchile.cl

ABSTRACT

We report the case of a 3-year-old girl, who is the third child of non-consanguineous parents with short stature, hypertrophic cardiomyopathy and mild dysmorphic features; all suggestive of Noonan syndrome. In addition, the patient presents with feeding difficulties, deep palmar and plantar creases, sparse hair, and delayed psychomotor and language development, all characteristics frequently observed in Cardio-facio-cutaneous syndrome. Molecular analysis of the Ras/MAPK pathway genes using high resolution melting curve analysis and gene sequencing revealed a *de novo KRAS* amino acid substitution of leucine to tryptophan at codon 53 (p.L53W). This substitution was recently described in an Iranian patient with Noonan syndrome. The findings described in the present report expand the phenotypic heterogeneity observed in RASopathy patients harbouring a *KRAS* substitution, and advocate for the inclusion of genes with low mutational frequency in genetic screening protocols for Noonan syndrome and other RASophaties.

Key words: Noonan syndrome, Cardio-facio-cutaneous syndrome, *KRAS* mutations

INTRODUCTION

The term “RASopathies” refers to a group of human syndromes caused by germline mutations in genes that encode components of the Ras/MAPK signalling pathway.[1] These syndromes share phenotypic features such as characteristic facies, growth retardation, congenital heart defects, developmental delay, learning disabilities, cutaneous abnormalities, cryptorchidism and a predisposition to malignancies.[2] RASopathies include Noonan syndrome (NS, MIM 163950), Noonan syndrome with multiple lentigines (MIM 115100), Costello syndrome (CS, MIM 218040) and Cardio-facio-cutaneous syndrome (CFCS, MIM 115150). As the different syndromes exhibit overlapping clinical features, sometimes it may be difficult to make a specific diagnosis based exclusively on clinical characteristics. The most frequent RASopathy, Noonan syndrome, has an incidence of 1 / 1,000 - 2,500 live births,[3] but this may be an underestimate due to patients with oligosymptomatic forms of the syndrome. Therefore, some of these patients may not be recognized during their entire life.[2] Germline mutation in four genes account for almost 67% of the patients with the clinical diagnosis of NS: *PTPN11*, *SOS1*, *RAF1* and *KRAS*.[4] The small GPTases RAS (HRAS, KRAS, and NRAS) are central components of the Ras/MAPK signal transduction pathway. These monomeric GTPases act as binary switches, cycling between an active, GTP-bound, and an inactive, GDP-bound state. In its active state, RAS interacts with and regulates diverse downstream effectors including RAF kinases (B-RAF, RAF1); phosphatidylinositol 3-kinase (PI3K), and RALGDS.[5]

Germline *KRAS* mutations account for approximately 3% of NS cases and 7% of all RASopathies including CFCS and a few individuals with a phenotype suggesting CS,[6] which reflects its complex genotype–phenotype correlation. In this study, we document the presence of a recently reported *KRAS* substitution[7] in a 3-year-old girl with a phenotype suggestive of Noonan syndrome.

CLINICAL REPORT

The patient is the third child of young non-consanguineous parents with no family history of birth defects. Her two older brothers are healthy. During her pregnancy the mother had urinary tract infections that required hospitalization. A fetal ultrasound performed at 35 weeks gestation showed pulmonary valve stenosis. She was born via C- section at 36 weeks gestational age with a birth weight of 3.5 kg (> 90th percentile), birth length 47 cm (> 50th percentile) and head circumference of 35.5 cm (> 90th percentile). She had transient hypoglycemia. A postnatal echocardiography exhibited right ventricle hypertrophy with premature closure of the ductus arteriosus. During her first months of life she exhibited apnea, failure to thrive and psychomotor delay. A cardiac catheterization at 2 months of age confirmed pulmonary valve stenosis, which was treated with a balloon valvuloplasty resulting in a residual subvalvar pulmonary gradient secondary to hypertrophic cardiomyopathy. Since the neonatal period she has had feeding difficulties, gastroesophageal reflux with failure to thrive and malnutrition. She underwent a gastrostomy with Nissan fundoplication during her first year of life.

However, she continued to have poor weight gain and growth velocity, placing her below the 5th percentile for chronological age.

Physical examination at 5 months of age showed a hypotonic, hypoactive and undernourished infant that was not tracking and had strabismus and epicanthal folds. She had mild dysmorphic features (Fig. 1, Table 1), slightly over folded helicies, deep palmar and plantar creases, soft skin, and sparse hair. She has a hemangioma (2 cm x 2 cm) in the cranial right vertex that was confirmed with cerebral magnetic resonance. In this exam there were no signs of meningo-angiomatosis.

She has been followed regularly by a multidisciplinary team with early intervention for her psychomotor and language delay.

Her karyotype is 46,XX and no pathogenic variants were found in the *PTPN11*, *SOS1* and *RAF1* genes. However, one missense substitution was documented in the *KRAS* gene.

MATERIALS AND METHODS

Ethical statement

This study, as well as the Informed Consent for DNA extraction, was approved by the Ethics Committee of Central Metropolitan Health Service in Santiago, Chile. Informed written consents were obtained from patient's parents for the study and photographs.

Point mutation screening

Point mutations in *PTPN11* (NM_002834.4), *SOS1* (NM_005633.3), *KRAS* (NM_004985.4) and *RAF1* (NM_001354689.1) genes were screened by High Resolution Melting (HRM) analysis. Briefly, exons frequently associated with RASopathies were amplified with specific primers (Supplementary Table S1). The PCR conditions were 1 x HOT FirePol® Eva Green® HRM Mix (Solis BioDyne, Estonia) or 1x SensiFAST HRM Mix (Bioline, UK), 0.25 - 1 μM each oligonucleotide and 15 ng genomic DNA in a total volume of 10 ul. The annealing temperatures for the amplification of the different exons are described in Supplementary Table 1. Amplification and melting curve analyses were performed in an Eco Real-Time PCR System (Illumina, San Diego, California, USA) and those exons with abnormal profiles relative to control samples (at least three) were sequenced bi-directionally in an ABI3730XL sequence analyser (Applied Biosystems, Foster City, CA, USA).

KRAS protein modelling

The primary structure of KRAS was used as a query sequence to scan against the specially curated nr20 (no sequences with >20% mutual sequence identity) protein sequence database with HHblits. The search produced an alignment between KRAS and homologous proteins, and highlighted conserved residues in the protein family. Homologous proteins with known structure were identified by using the Phyre2 homology-recognition server V 2.0.[8] The sequence alignment produced by Phyre2 for the highest-scoring hit (PDB ID 1X1R) was analysed visually to highlight the conservation of structurally and functionally important amino acid residues. The model of KRAS was validated with Coot [9] and through visual inspection by using the 3D graphics software Pymol (Schrödinger.com). Single substitutions were created using Coot and

validated as mentioned above. These programs revealed that the structure models needed no further modifications.

RESULTS

Screening of nucleotide changes by high resolution melting curve analysis showed an abnormal profile of *KRAS* exon 3 amplicon from the patient's genomic DNA (Supplementary Fig. S1). Sanger DNA sequencing revealed a heterozygous thymine to guanine change at position 158 (c.158 T>G). The substitution affects codon 53 (T**T**G > T**G**G) which leads to a leucine to tryptophan amino acid substitution (p.L53W) (Fig. 2a). This substitution was not detected in the patient's parents (maternity and paternity were not confirmed) which suggests a *de novo* event (Fig. 2b). Furthermore, the c.158T>G substitution was not detected in 100 healthy controls after allele-specific PCR analysis (Supplementary Fig. S2). To date, the substitution p.L53W has not been reported in well-established reference databases including ExAC, 1000 Genomes, Ensembl and NCBI.

This substitution is predicted to be either probably damaging (score of 0.996 - sensitivity: 0.36; specificity: 0.97) or damaging (score 0.00) according to PolyPhen-2[10] and SIFT, respectively. Importantly, the leucine residue at position 53 of KRAS is conserved among evolutionary distant species (Fig. 2c) and across RAS family members. A structure model of p.L53W was produced to study the plausible consequence of this substitution on KRAS protein structure. Although seven rotamers of tryptophan are possible, Fig. 2d (up) shows the two most likely rotational isomers of p.W53 as judged

by geometry (e.g., chi angle) constrains and the absence of steric clashes with neighbor amino acid residues. In both cases the introduction of this bulky hydrophobic amino acid in the small cleft formed by the β1, β2 and β3-strands and the α1 and α5-helix is predicted to induce local conformational changes to avoid steric clashes among residues located in the vicinity.

DISCUSSION

We report a *KRAS* missense substitution (p.L53W) in a patient with clinical features suggestive of Noonan Syndrome, such as characteristic facies (epicanthal folds, low-set ears and ptosis), hypertrophic cardiomyopathy and growth retardation. The patient also presented with feeding difficulties, deep palmar and plantar creases, sparse hair, sparse eyebrows and psychomotor and language delay, all characteristics that are common in CFC syndrome patients and unfrequented in NS patients (Table 1). The co-occurrence of features of both syndromes in patients with *KRAS* mutations has been described previously[11-13] (Table 1) and demonstrated that specific diagnosis based exclusively on clinical characteristics is difficult in patients with *KRAS* pathogenic variants.

Recently, Tafazoli and collaborators[7] reported a L53W amino acid residue substitution in a patient with a similar phenotype to our patient. Our studies confirm this association and show that: i) the p.L53W substitution was not detected in her relatives (*de novo*) nor in 100 healthy controls; ii) the amino acid substitution affects a residue in a position that is conserved across the RAS family, including the recently NS associated gene *RIT1*[14]; and iii) that different predictive tools (Poly-Phen and SIFT) classified this substitution as

a probably damaging or damaging amino acid residue variant. Taken together, these observations, the patient phenotype, and her clinical evolution led to the classification of this variant as Probably Pathogenic, according to The American College of Medical Genetics and Genomics (ACMG) classification guidelines.[15]

Even though an *in silico* structure model of the KRAS p.L53W mutant has been reported,[7] the specific amino acid residues or secondary structural elements (α-helix or β-strand) whose relative position could be affected by the substitution were not described, nor a mechanistic hypothesis proposed to explain the effects of the substitution on protein function and/or protein stability. We addressed this gap in knowledge and propose a 3D structure model of the pL53W mutant. Our structure model suggests that different residues that are located in close proximity to p.L53W can undergo important conformational changes to accommodate the bulkier tryptophan amino acid residue in the small cleft defined by the β1-β2-β3 strands and the α1 and α5 helices (magenta residues in Fig. 2d). None of the residues of the small cleft have previously been associated with pathogenic substitutions (somatic or germline) or analysed *in vitro* or *in vivo* to determine the functional consequences of the substitutions. Since members of the RAS protein family (eg, KRAS, NRAS, HRAS) present a conserved peptide sequence,[5] we surveyed for reported mutations affecting residues in equivalent positions across the RAS family members HRAS and NRAS. In 2011 Runtuwene and coworkers[16] described a patient with Noonan syndrome with a p.I24N substitution in NRAS. The authors showed that the NRAS p.I24N mutant affected the GTP bound (active) form, which resulted in much higher MAPK phosphorylation activity compared to the wild type protein. The p.I24N mutant would result in a steric

repulsion between the α1-helix and the β2-strand. This in turn destabilizes the guanine nucleotide binding pocket resulting in an increased GDP to GTP exchange rate due to a 9:1 ratio of GTP:GDP in the cell. Based on this evidence, the NRAS p.I24N substitution was classified as a mild activation mutation. Similar to residue leucine 53, the isoleucine at position 24 is conserved between NRAS and KRAS. In the wild type KRAS crystal structure the distance between p.I24 and p.L53 is 6.9 Å, whereas the p.L53W substitution with the most likely tryptophan rotamer is expected to reduce the distance to 2.1 Å (Fig. 2d - down). This would produce a strong repulsing force between the side chains of the residues that define the α1-helix and the β3-strand, resulting in important conformational changes in the vicinity of the GTP-binding pocket. We postulate here that the p.L53W substitution is a mild activated KRAS mutant similar to that reported for the NRAS p.I24N mutant. To the best of our knowledge, to date only four NS patients with the *NRAS* p.I24N mutation have been described. Those patients share some distinctive features with our patient because three of them exhibited hypertrophic cardiomyopathy and one had a hemangioma. In the patient we examined, a detailed cardiac study showed prenatal right ventricle hypertrophy with premature closure of the ductus arteriosus and subsequent postnatal confirmation of pulmonary valve stenosis and hypertrophic cardiomyopathy. In agreement with our findings, Tafazoli and collaborators reported pulmonary valve stenosis in the other patient with the *KRAS* p.L53W substitution.[7]

In conclusion, this report provides further evidence of one recently reported *KRAS* pathogenic variant with Noonan syndrome, and thus expands the variety of pathogenic *KRAS* variation associated with RASopathies. We also propose a structure-guided

mechanistic explanation of the contribution of this substitution in Noonan syndrome. Finally, confirmation of the clinical diagnosis in this patient demonstrates the importance of the inclusion of genes with low mutational frequency in genetic screening protocols for Noonan syndrome and other RASopathies. These findings emphasise the need to explore further the potential of modern techniques, such us targeted gene panel sequencing, for the diagnosis of syndromes associated with mutations in genes of the Ras/MAPKpathway.

NOTE

Written informed consent was obtained from the patient's mother for publication of this case report and accompanying images.

CONFLICT OF INTEREST

None.

ACKNOWLEDGMENTS

We are grateful to the patient and her family for helping us to perform this study. This work was supported by Fondecyt Grant 1140450 to F.R.

REFERENCES

1 Tidyman WE & Rauen KA. The RASopathies: developmental syndromes of Ras/MAPK pathway dysregulation. Curr Opin Genet Dev. 2009; 19: 230-236.

2 Rauen KA. The RASopathies. Annu Rev Genomics Hum Genet. 2013; 14: 355-369.

3 Romano AA, Allanson JE, Dahlgren J, et al. Noonan syndrome: Clinical features, diagnosis, and management guidelines. Pediatrics 2010; 126: 746–759.

4 Aoki Y, Niihori T, Inoue S, Matsubara Y. Recent advances in RASopathies. J Hum Genet. 2016; 61: 33-39.

5 Vetter IR, & Wittinghofer A. Signal transduction–the guanine nucleotide-binding switch in three dimensions. Science 2001; 294: 1299–1304.

6 Brasil A, Malaquias A, Kim C, et al. *KRAS* Gene Mutations in Noonan Syndrome Familial Cases Cluster in the Vicinity of the Switch II Region of the G-domain: Report of Another Family With Metopic Craniosynostosis. Am J Med Genet A. 2012; 158A: 1178-1184.

7 Tafazoli A, Eshraghi P, Pantaleoni F, et al. Novel mutations and their genotype-phenotype correlations in patients with Noonan syndrome, using next-generation sequencing. Adv Med Sci. 2017; 63: 87-93.

8 Kelley LA, Mezulis S, Yates CM, Wass MN, Sternberg MJ. The Phyre2 web portal for protein modeling, prediction and analysis. Nature Prot 2015; 10: 845-858.

9 Emsley P, Lohkamp B, Scott WG, Cowtan K. Features and Development of Coot.

Acta Cryst Section D - Biological Crystallography. 2010; 66: 486-501

10 Adzhubei IA, Schmidt S, Peshkin L, et al. A method and server for predicting damaging missense mutations. Nat Methods 2010; 7: 248-249.

11 Carta C, Pantaleoni F, Bocchinfuso G, et al. Germline missense mutations affecting KRAS Isoform B are associated with a severe Noonan syndrome phenotype. Am J Hum Genet. 2006; 79: 129-135.

12 Zenker M, Lehmann K, Schulz AL, et al. Expansion of the genotypic and phenotypic spectrum in patients with *KRAS* germline mutations. J Med Genet. 2007; 44: 131-135.

13 Razzaque MA, Komoike Y, Nishizawa T, et al. Characterization of a novel *KRAS* mutation identified in Noonan syndrome. Am J Med Genet A. 2012; 158A: 524-532.

14 Cavé H, Caye A, Ghedira N, et al. Mutations in *RIT1* cause Noonan syndrome with possible juvenile myelomonocytic leukemia but are not involved in acute lymphoblastic leukemia. Eur J Hum Genet. 2016; 24: 1124-113

15 Richards S, Aziz N, Bale S, et al. Standards and guidelines for the interpretation of sequence variants: a joint consensus recommendation of the American College of Medical Genetics and Genomics and the Association for Molecular Pathology. Genet Med. 2015; 17: 405-424.

16 Runtuwene V, van Eekelen M, Overvoorde J, et al. Noonan syndrome gain-of-function mutations in *NRAS* cause zebrafish gastrulation defects. Dis Model Mech. 2011; 4: 393-399.

FIGURE LEGENDS

Fig. 1: Facial photographs of patient at five months (a) and three years (b) of age showing hypertelorism, epicanthal folds, mild ptosis, sparse hair and low set ears.

Fig. 2: *KRAS* missense mutations. **a**) Sequence analyses of the *KRAS* exon 3 shows a heterozygous base substitution of thymine c.158 by guanine in the patient. A wild type reference sequence is shown. The black line under the nucleotides sequence highlights the codon 53 (NM_004985.4). **b**) Pedigree chart of the patient, where genotype for nucleotide c.158 (T/T or T/G) is shown for each family member, as well as the corresponding chromatogram. **c**) Amino acid sequence alignment of the human *KRAS* strand 3 (β3, amino acid residues 51 to 60) with the orthologues from different species, where the amino acid residue leucine 53 is indicated with arrows. Secondary structure organization diagram of *KRAS* showing the position of β3, the substitution p.L53W, and two NS associated residues substitutions that are close to p.L53. Both switch regions (SW I and SW II) and the hypervariable region (HVR) are also shown. **d**) [up] Three-dimensional structure of the *KRAS* protein with two possible rotamers of p.W53 (purple and green side chains). Residues affected by the p.L53W substitution are show in magenta. [down] Atom distances between p.I24 and p.L53 (left) or p.W53 (right) side chains.

Figure 1

a

b

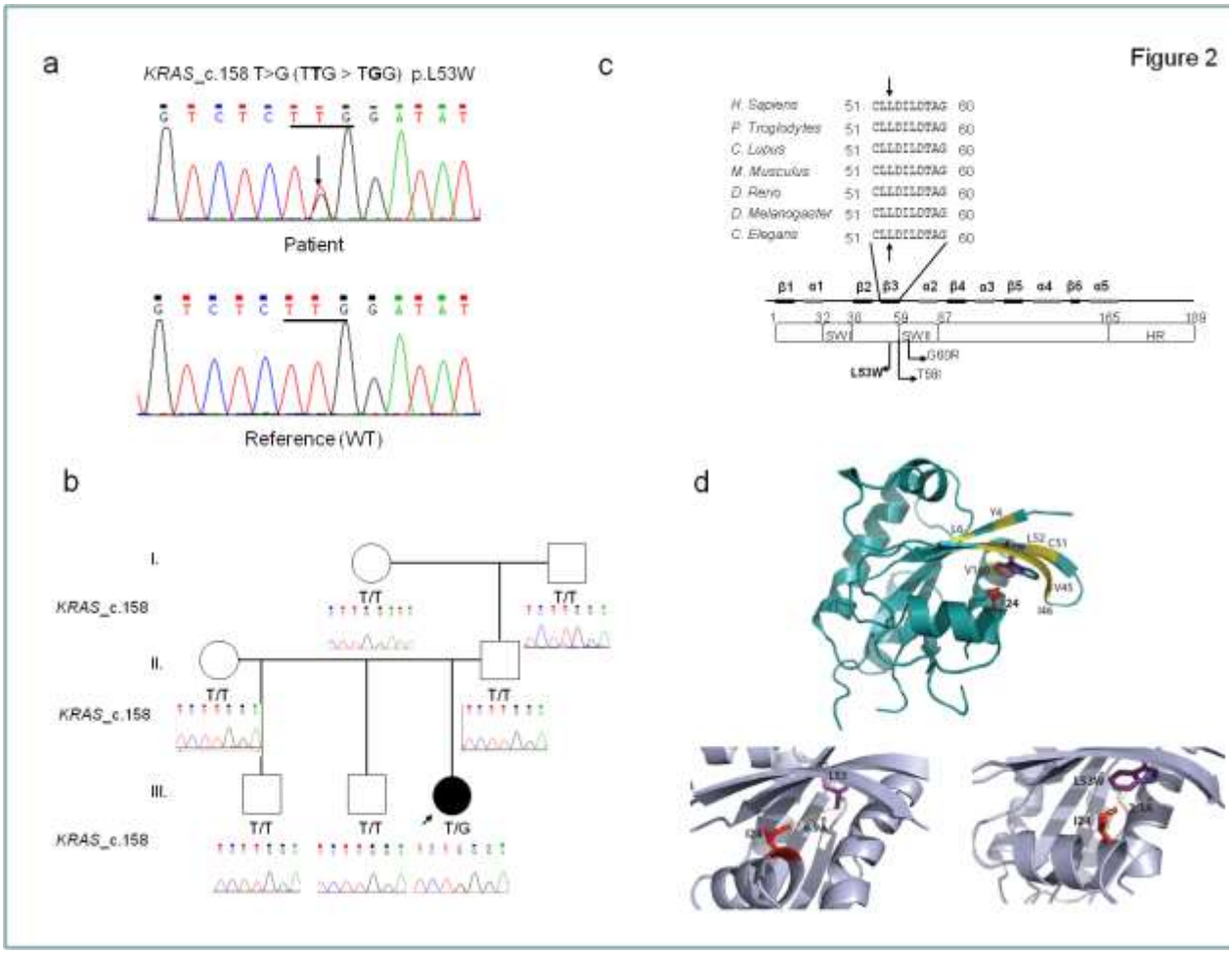
a
KRAS_c.158 T>G (TTG > TGG) p.L53W
Patient
Reference (WT)
b
I.
II.
III.
KRAS_c.158
T/T
T/G
c
H. Sapiens
P. Troglodytes
C. Lupus
M. Musculus
D. Rerio
D. Melanogaster
C. Elegans
β1 α1 β2 β3 α2 β4 α3 β5 α4 β6 α5
SWI
SWII
HR
G60R
L53W
T58I
d

Figure 2

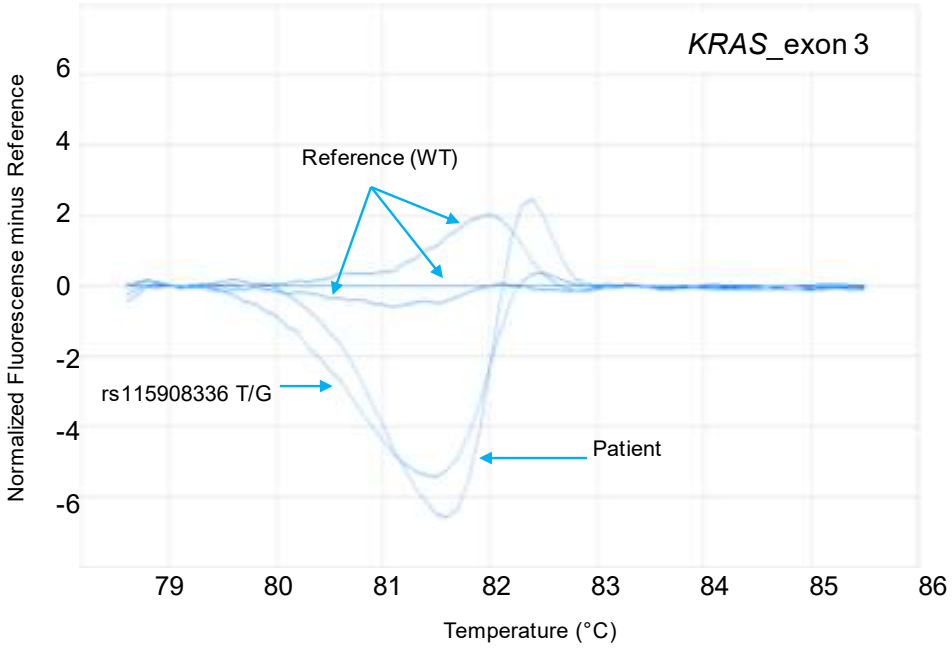

Result of the HRM analysis for *KRAS* exon 3 in patient, reference samples (wild type - WT) and controls with known nucleotide changes (rs115908336 T/G).

Supplementary Fig. S2

Allele-specific PCR

Confirmation of a c.156 T>G substitution and analysis of healthy controls was performed by allele-specific PCR method. Briefly, genomic DNA (37,5 ng) was incubated with the forward primers KRAS-3_156T (5' *GGAGAAACCTGTCTCTT* 3') or KRAS-3_156G (5' *GGAGAAACCTGTCTCTG* 3') and the reverse primer KRAS-3R (CCTACCTCATAAACATTATTTAA 3'); 1X Green GoTaq® Flexi Buffer; 2 mM $MgCl_2$; 0.2 mM dNTPs and 1 unit of GoTaq® G2 Flexi DNA Polymerase; in a final volume of 15 µl. Amplification was performed in a T960 thermocycler (Hangzhou Jingle Scientific Instrument, China) with the following thermal cycles: 2 minutes at 95°C; 30 cycles of 30 seconds at 95°C, 30 seconds at 55°C and 30 seconds at 72°C; followed by a final extension of 5 minutes at 72°C. The PCR products were separated on a 2% agarose gel and stained with SYBR® Safe DNA Gel Stained (Invitrogen, OR, USA).

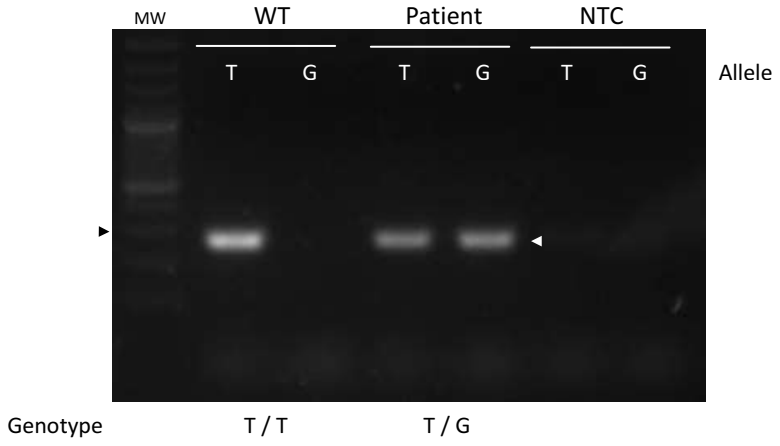

Result of allele-specific PCR for c.156 T>G substitution of *KRAS* exon 3 in reference sample (wild type - WT); Patient and non template control (NTC). Black arrowhead indicates 300 bp standard (MW) and white arrowhead depicts the ~ 270 bp amplicon.

Supplementary Table S1: Primers used for exon amplification

Genes	Exons	Primers sequence (5' > 3')	Annealing T° (°C)	Amplicon size (nt.)
PTPN11	2#	F: GTA GTG CTG ACA GTG TC TTG T R: CAG CAA GCT ATC CAA GCA TGG T	60	258
	3#	F: CGA CGT GGA AGA TGA GAT CTG A CAG TCA CAA GCC TTT GGA GTC AG	TD_ 70 - 62	384
	4#	F: ACA ACA TGA ACC CAT AGT AGA GC R: CAG AAA AAT CAC CCA AAG GTA	58	350
	7#	F: GAA CAT TTC CTA GGA TGA ATT CC R: GGT ACA GAG GTG CTA GGA ATC A	60	271
	8#	F: GAC ATC AGG CAG TGT TCA CGT TAC R: CCT TAA AGT TAC TTT CAG GAC ATG	60	350
	12#	F: GCT CCA AAG AGT AGA CAT TGT TTC R: GAC TGT TTT CGT GAG CAC TTT C	60	250
	13#	F: TCA TCC TGG CTC TGC AGT TTC TCT R: CGT ATC CAA GAG GCC TAG CAAG	66	262
SOS1	6#	F: AAA TGA CTT ATT GGC TCA AAA T R: TTA GTA TCT ATG ACT TTA GCT GGA A	TD_ 60 - 52	324
	7#	F: TTG TGC TCG CAT AGT CGT G R: GGA GAC AGT GGT AAA CAG GG	65	357
	8#	F: CGA CCT GGT TTT CAT GAT R: ACT AAT GTG CAG GGT ACT CA	60	300
	10.1*#	F: AAT CTA CTT TTA CAC TTT CCC R: TAA TTT GTA CCT TTC GCA TA	54	388
	10.2*#	F: TTG GAC AGT GTT GTA ATG AAT TT R: CTC ATC TGC TCC TCT TTC TC	54	394
	10.3*#	F: TAG TGT TAT ATT TTC TGC CAA G R: AGT TTC TTT TCT ATT TTA GGC AC	54	390
	11#	F: TTC TAC TTG GCA AAA CAT T ATT TCT GAA AAG GAT CTT AGC	TD_ 60 - 52	285
	12#	F: AAA CGT TTG TGG TTT TCT ATT TG R: TTT ATT GTC ACC CCT CTC	54	300
	16#	F: AAA TTC TTT AAG CTA TAA CTT TA R: ACC AAT TCA TTA CAA AAC TTA G	TD_ 60 - 52	386
RAF1	7#	F: GCC CTT AAG CAT CTT ACT TAG TC R: TGA AAC CCA AAA CTC TGA AAT AA	60	330
	12#	F: GGG AAA GCA CAG TAG ACC TC R: ACAGAATCGCTTAATGGACTAGA	56	348
	14$	F: GTG TTA TAA AGA ACT TTG GGA TA R: CTA GGG GTC ATG TGG ATT	54	317
	17#	F: AGG GTA CAT CCT GTG TCT TTG AG R: AGG GAG CAG AAA AGT GGT G	60	275
KRAS	2$	F: ATT AAC CTT ATG TGT GAC ATG TT R: CCT TTA TCT GTA TCA AAG AAT G	54	242
	3$	F: ATA ACA CCT TTT TTG AAG TAA A R: CCT ACC TCA TAA ACA TTA TTT AA	TD_ 56 - 48	369
	6$	F: GAA GAG AAA CAT AAA GAA TCC R: GTG TAA TGT ACA AAA ATT ACC AC	54	293

F: forward; **R**: reverse; **nt**.: nucleotides; **TD**: touchdown technique, ***** exon 10 is analyzed in three fragments,
HOT FirePol® Eva Green® HRM Mix, $ SensiFAST HRM Mix.